A GNSS Receiver Interference Suppression Technique based on Wavelet Packet Transform

Jian Huang[1, a], Yong Xu[2, b] and Qing Chang[1, c]

[1] School of Electronic and Information Engineering, Beihang University, No. 37 Xueyuan Road, Haidian District, Beijing 100191, China

[2] Institute of Unmanned Systems Research, Beihang University, No. 37 Xueyuan Road, Haidian District, Beijing 100191, China

[a] ajiankaishui@163.com, [b] xuyong1518@163.com, [c] changqing@buaa.edu.cn

Keywords: global satellite navigation system; wavelet packet transform; interference suppression; adaptive algorithm.

Abstract: Global navigation satellite systems (GNSSs) have been widely used in military and civil fields, and the security and application of GNSSs have been greatly weakened by various intentional and unintentional interference. An interference suppression technique based on wavelet packet transform (WPT) is proposed in this paper, which can effectively suppress interference in the same frequency band of the GNSS receiver. First, we introduce the principles and implementation of WPT. The anti-jamming performance of the proposed method is evaluated according to the carrier-to-noise ratio (CNR) at the receiving end. Additionally, the differences in the anti-jamming performance of the proposed algorithm for different types of interference are analyzed. In a case where the spread spectrum code rate is 2.046 MHz, for the pulse interference shown in Table 2, the maximum interference-to-signal ratio (ISR) that can be suppressed by the proposed method is 100 dB. For sweep interference, the maximum ISR that can be suppressed is 80 dB, and for single-tone interference, the maximum ISR that can be suppressed is 80 dB.

1. Introduction

GNSSs can provide accurate PVT (Position, Velocity, Time) information on a global scale and play a very huge role in the economy, military field, transportation and other fields [1]. Most GNSSs adopt a direct sequence spread spectrum (DSSS) communication system; although it has a certain anti-jamming ability, in complex electromagnetic environments, the navigation satellite is at an altitude of more than 20,000 kilometers, and the signal arrives after long-distance transmission. The power of the satellite signal that arrives on the ground is approximately -130 dBm or even lower and is already very weak [2]. The CNR is approximately -20dB when the power intensity of some other signals in the navigation signal band exceeds the interference tolerance of the receiver, the CNR deteriorates sharply, the receiver may easily lose the lock on the satellite signal, and finally the positioning cannot be achieved.

In recent decades, scholars in related fields have performed a large amount of research on GNSS interference suppression techniques. To date, a large number of classic and effective interference suppression methods have emerged, and some of them are introduced as follows. All the methods mentioned in this paper are based on a single-antenna, and array-antenna methods are beyond the scope of this paper and are not introduced. In summary, the commonly used methods to suppress interference include time-domain adaptive filtering, code-aided techniques, frequency-domain adaptive filtering and methods based on neural networks [3].

In Ref [4], time-domain adaptive filtering and code-aided techniques before 2000 have been summarized. Time-domain adaptive filtering includes finite impulse response filter (FIR) and infinite impulse response notch filter (IIR) structures, and time-domain adaptive filtering can only suppress narrow-band interference (NBI) stationary signals. An adaptive FIR filter's basic idea is to exploit

the discrepancy of narrowband signals and wideband signals to form an accurate replica of the NBI that can be subtracted from the received signal to suppress the NBI [5]. In Refs [6,7], the performance of a linear prediction filter and linear interpolation filter were analyzed in detail. The least mean square (LMS) algorithm and recursive least squares (RLS) algorithm are commonly used adaptive algorithms. The traditional LMS algorithm has a fixed step size, and the key for the algorithm is the selection of step sizes. In Ref [8], an LMS adaptive filter with variable step sizes was proposed, which improves the convergence speed and steady error compared with the traditional algorithm. An improved RLS algorithm with variable forgetting coefficients was proposed in Ref [9], and has a smaller mean square error and smaller bit error rate than the traditional LMS and RLS algorithms. Adaptive FIR filter usually has a better suppression effect on single-tone interference, and the performance of multi-tone interference, pulse interference, sweep frequency interference and Gaussian NBI will deteriorate. An IIR notch filter has better adaptive performance than a FIR filter, and can effectively suppress single-tone interference, multi-tone interference, Gaussian NBI, etc. In Ref [10], the author proposes a second-order adaptive IIR notch filter with a lattice structure applied to a GPS receiver for interference detection and suppression, which can suppress multi-tone interference by cascading multiple second-order IIR notch filters. Code-aided techniques exploit the knowledge of multi-user detection technology, which can effectively transform NBI into multiple virtual users. In Refs [11,12], the author introduces the principle of a code-aided technique, and its performance is analyzed by simulation.

Transform domain adaptive filtering is a nonparametric interference suppression technique. Using a frequency domain interference suppression algorithm will reduce the influence of narrow-band interference. The interference suppression takes place in the frequency domain after which the signal is transformed back to the time domain, where the rest of the signal processing is performed. The transform from the time domain to the frequency domain and vice versa are made by FFT and IFFT, respectively. In Ref [13], a method based on the mean and variance of Fast Fourier Transform (FFT) results is proposed to calculate the interference threshold. In Ref [14], an n-sigma algorithm is proposed, which calculates the logarithm of FFT results and then calculates the mean and variance of the logarithm results. This algorithm can determine the threshold more stably and accurately. In Ref [15], a time-frequency analysis method is proposed, that combines an IIR notch filter and short-time Fourier transform (STFT) to find the interference spectrum, and the coefficient of the IIR notch coefficient can be found. Although FFT and STFT can quickly locate the frequency band where the interference is located, they have inherent defects. Signal truncation will cause spectrum leakage, and FFT calculation of limited sampling points will bring spectrum resolution problems [16]; these defects limit the application of FFT and STFT.

WPT is a rather novel method for analyzing a time series, and formal research can be traced back to the 1980s [17]. Different from FFT and STFT, WPT has excellent time-frequency analysis ability, can highlight local features of a signal, and is very suitable for interference detection and suppression in GNSSs. A fast WPT algorithm is the Mallat algorithm, which forms a binary decomposition tree by symmetrically decomposing a signal spectrum layer by layer to achieve equivalent spectrum sub-band division [17]. In Refs [18-20], an optimal wavelet packet decomposition tree based on a cost function is adopted for interference detection and suppression. The energy compaction measurement and the sub-band power ratio (SPR) are used to identify the interference sub-bands.

In this paper, we propose an adaptive interference suppression method based on WPT in GNSS receivers. Different from the methods proposed in most references, we select an appropriate decomposition layer according to the signal spectrum bandwidth to completely decompose the signal. This method has low computational complexity and good anti-interference performance. We analyze the effect of different decomposition layers on the anti-interference performance, and then choose an optimal decomposition layer. Based on acquisition performance and the CNR results, the performance of an anti-jamming scheme to suppress different interference is verified and evaluated. Finally, we compare and analyze the proposed method with other typical interference suppression techniques and further clarify the characteristics and advantages of the proposed method.

The outline for the rest of this paper is as follows. Section 2 presents the signal model and adaptive interference suppression algorithm and introduces the effect of the decomposition layer on acquisition performance. And the complete signal processing process is described in section 2. The simulation and analysis are presented in section 3. A brief conclusion is presented in the last section.

2. Signal Model and Interference Suppression Algorithm

In this section, we introduce the signal model and describe the interference suppression method in detail. We first introduce some concepts of the signal model, orthogonal wavelet packet decomposition and reconstruction theory, and then, we describe the anti-jamming algorithm.

2.1 Signal Model

For a single-antenna receiver, the intermediate frequency (IF) signal affected by white Gaussian noise and interference signals at the receiving end can be expressed as [21]

$$r(t) = s(t) + n(t) + j(t) = \sum_{i=1}^{I} s_i(t) + n(t) + j(t) \tag{1}$$

where I represents the number of visible navigation satellites. $s_i(t)$ is the i-th visible satellite signal, and $n(t)$ and $j(t)$ denote additive white Gaussian noise and interference signals, respectively. $s_i(t)$ can be expressed as follows:

$$s_i(t) = \sqrt{2P_i}c_i(t-\tau_i)d_i(t-\tau_i)\cos[2\pi(f_{IF}+f_{d,i})t+\varphi_i] \tag{1}$$

where P_i represents the signal power of the i-th visible satellite, $c_i(t)$ and $d_i(t)$ are the spread spectrum code and navigation data flow of the i-th visible satellite, respectively, τ_i is the code delay introduced by the propagation channel, f_{IF} is the IF, and $f_{d,i}$ and φ_i denote the carrier Doppler frequency and phase of the i-th visible satellite, respectively.

We model single-tone interference, sweep interference and pulse interference, and their expressions are as follows:

Single-tone interference:

$$j_{\text{single}}(t) = A \cdot \cos(2\pi f_{IF} t + \varphi_j) \tag{2}$$

Sweep interference:

$$j_{chirp}(t) = A \cdot \cos\left\{2\pi \cdot [(f_{IF} - \frac{B_{chirp}}{2}) + \frac{B_{chirp}}{T_{chirp}} \cdot (t \bmod T_{chirp})] \cdot t + \varphi_j\right\} \tag{3}$$

Pulse interference:

$$j_{\text{pus}}(t) = \begin{cases} A\cos(2\pi f_{IF} t + \varphi_j) & t \bmod T_{chirp} < R_{duty} \cdot T_{chirp} \\ 0 & others \end{cases} \tag{4}$$

where A denotes the interference signal amplitude, φ_j is the initial phase of the interference signal, B_{chirp} and T_{chirp} denote the bandwidth and period of the sweep interference, respectively, R_{duty} denotes duty ratio of the pulse interference, and mod denotes the modulo operation. The power spectral density of the three types of interference is shown in Fig. 1.

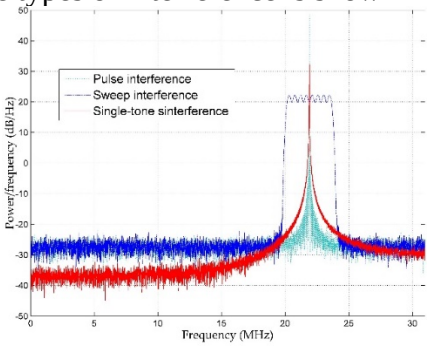

Fig. 1 Power spectral density

After down-conversion to IF, the GNSS signal is converted into a digital signal by an A/D converter. The digital signal model can be expressed as follows:

$$r = s + n + j \tag{5}$$

where

$$r = [r[k], r[k+1], \ldots, r[k+N-2], r[k+N-1]] \tag{6}$$

$$n = [n[k], n[k+1], \ldots, n[k+N-2], n[k+N-1]] \tag{7}$$

$$j = [j[k], j[k+1], \ldots, j[k+N-2], j[k+N-1]] \tag{8}$$

N denotes the consecutive samples starting from time instant k.

2.2 Wavelet Packet Decomposition and Reconstruction

Wavelet packet operations include decomposition and reconstruction. For $l = 0,1,2\ldots$, we obtain the following coefficient:

$$d_{j,n}^{(l)} = \int_R f(t)\bar{\mu}_{l,j,n}(t)\mathrm{d}t \tag{9}$$

We can obtain the decomposition formula and reconstruction formula of the wavelet packet as follows:

Decomposition:

$$d_{j,n}^{(2l)} = \sum_{m\in Z} \bar{h}_{m-2n} d_{j+1,m}^{(l)} \tag{10}$$

$$d_{j,n}^{(2l+1)} = \sum_{m\in Z} \bar{g}_{m-2n} d_{j+1,m}^{(l)} \tag{11}$$

Reconstruction:

$$d_{j+1,m}^{(l)} = \sum_{n\in Z} \left(h_{m-2n} d_{j,m}^{(2l)} + g_{m-2n} d_{j,n}^{(2l+1)} \right) \tag{12}$$

The decomposition formula and reconstruction formula of the wavelet packet show the original signal's decomposition coefficients in

$$U_j^{2l} = closespan\left\{ \mu_{2l,j,n}(t) = 2^{\frac{j}{2}} \mu_{2l}(2^j t - n); n \in Z \right\} \tag{13}$$

and

$$U_j^{2l+1} = closespan\left\{ \mu_{2l+1,j,n}(t) = 2^{\frac{j}{2}} \mu_{2l+1}(2^j t - n); n \in Z \right\} \tag{14}$$

can be obtained from the decomposition coefficients of

$$U_{j+1}^{l} = closespan\left\{ \mu_{l,j+1,n}(t) = 2^{\frac{j+1}{2}} \mu_l(2^{j+1} t - n); n \in Z \right\} \tag{16}$$

and vice versa. The wavelet packet decomposition process shown in Fig. 2, and the synthesis process is the inverse process.

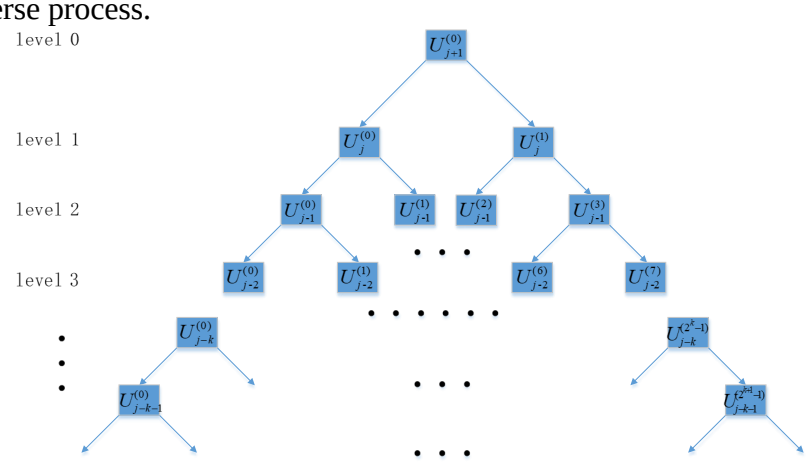

Fig. 2 Wavelet packet decomposition.

2.3 Signal Processing Process

Generally, the receiver has digital down conversion, A/D sampling and other modules behind the RF front end, and it processes the digital IF signal directly. The generated signal with noise and interference is processed as shown in Fig. 3, and the interference suppression module is in front of the acquisition and tracking module of the receiver and is shown in Fig. 4.

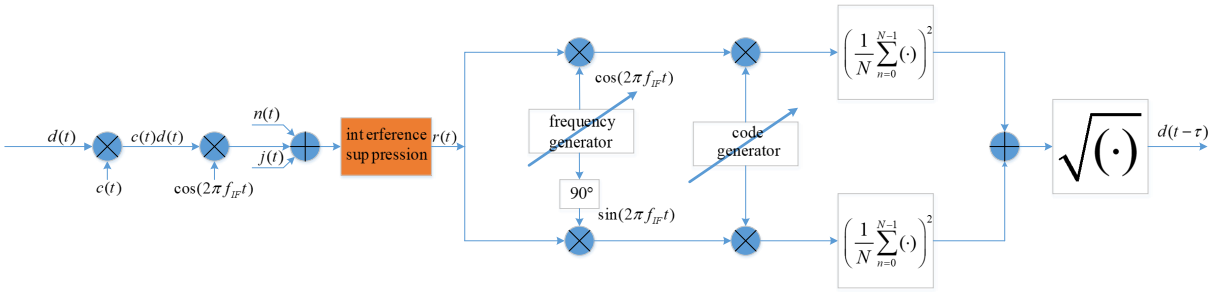

Fig. 3 Signal processing process block diagram

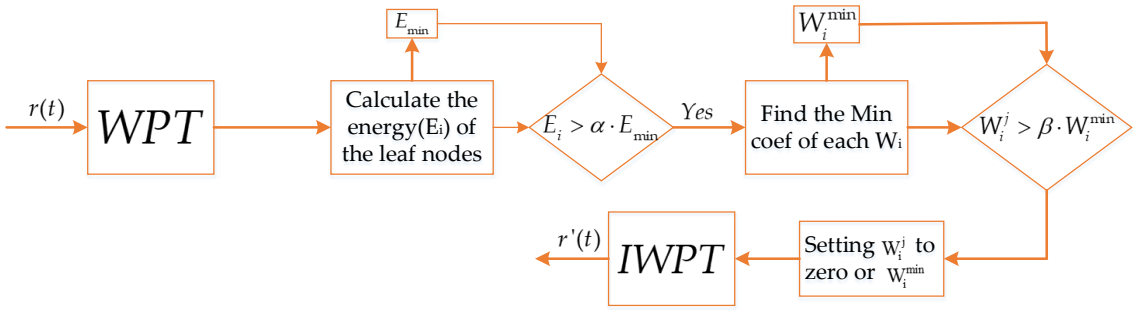

Fig. 4 Anti-jamming processing block diagram

In this scheme, the sampling rate is 62 MHz, the spread spectrum code rate is 2.046 MHz, and the IF is 40.098 MHz. The basic simulation parameters are listed in Table 1.

Table 1. Basic simulation parameters

Parameter	Value
Code Rate	2.046 MHz
Code Length	2046
IF	40.098 MHz
Sampling Rate	62 MHz
INR/CNR	-20 dB/46dB•Hz
Simulation Time	3000 ms

3. Simulation and Verification

In this section, the anti-interference performance of the proposed scheme is mainly verified and evaluated based on the acquisition and tracking performance of the receiver. In addition, according to the CNR at the receiving end, the performance of the proposed method in suppressing different types of interference is analyzed. The interference types are sweep interference, pulse interference and single-tone interference and their parameters are shown in Table 2.

Table 2. Interference parameters

Interference Type	Parameter	Value
Sweep Interference	Initial Frequency	38.052 MHz (40.098 MHz-2.046 MHz)
	Period	1ms
	Bandwidth	4.098 MHz (GNSS signal's bandwidth)
	Sweep Type	Linear
Pulse Interference	Period	1 ms
	Duty	0.1
Single-tone Interference	Frequency	40.098 MHz

3.1 Anti-jamming Performance with Difference Layer

In this subsection, we set three types of interference scenarios, as shown in Table 3, which are sweep interference, pulse interference, and single-tone interference with an ISR of 70 dB.

Table 3. Simulation scenario parameter settings

Scenario	ISR
Sweep Interference	70 dB
Pulse Interference	70 dB
Single-tone Interference	70 dB

Fig. 5 and Fig. 6 show the acquisition results and tracking CNRs of the receiver after interference suppression, respectively. As shown in Fig. 5, strong acquisition correlation peaks appear in all three scenarios, and the acquisition performance is excellent.

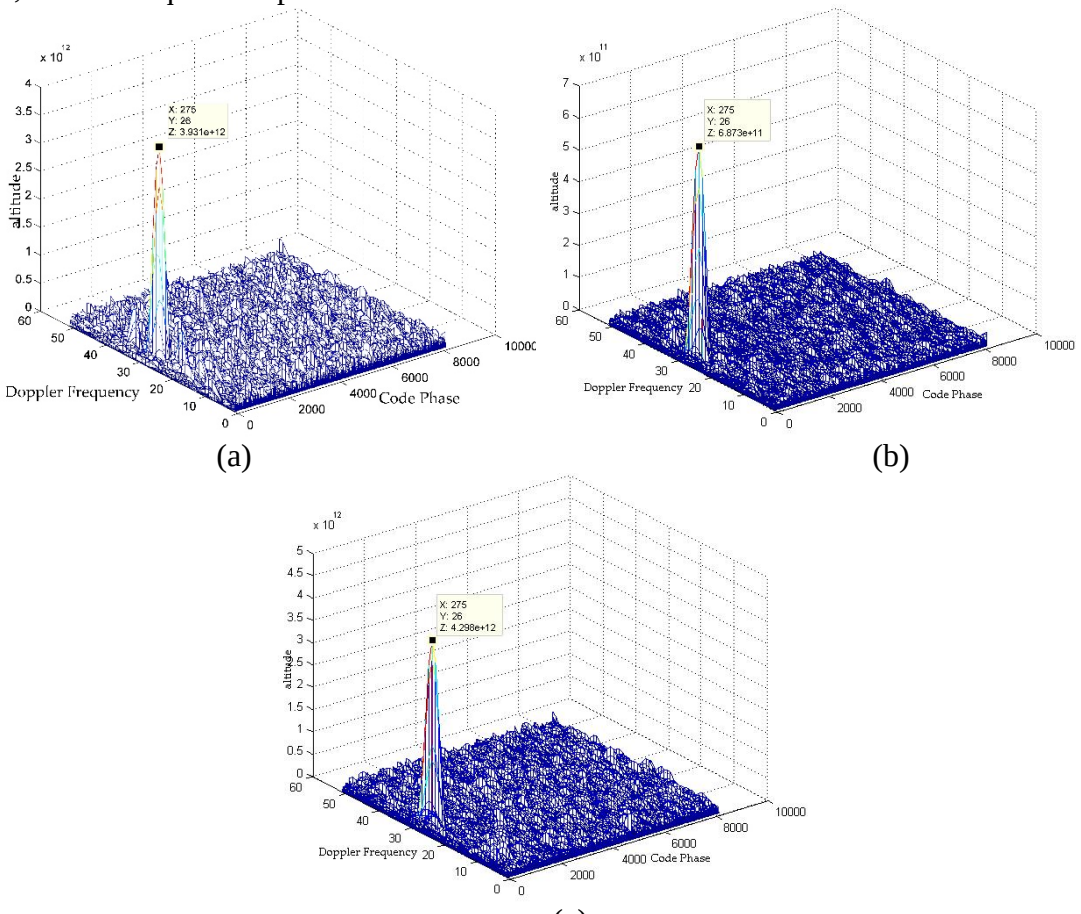

Fig. 5 Acquisition results diagram. (a) Sweep interference; (b) pulse interference; (c) single-tone interference.

As shown in Fig. 6, the CNR tends to be stable after 500 ms in all three scenarios. When the interference intensity is the same, after interference suppression, the attenuation of the CNR caused by pulse interference is the smallest, followed by sweep interference, and the single-tone interference is the worst. The scheme proposed in this paper has a better ability to suppress non-stationary interference than stationary interference.

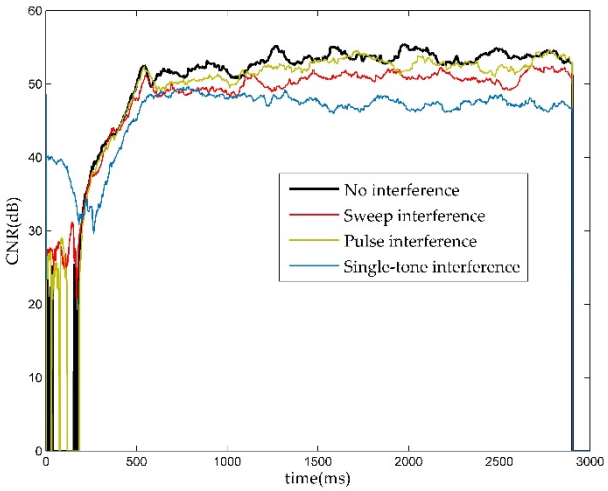

Fig. 6 Tracking CNRs for each interference

3.2 Anti-jamming Performance Verification and Evaluation

Similarly, in this subsection, three different types of interference are set up for simulation analysis, and different ISRs are set for each scenario. Fig. 7, Fig. 8 and Fig. 9 show CNR curves of sweep interference, pulse interference and single-tone interference with different ISRs after interference suppression, respectively.

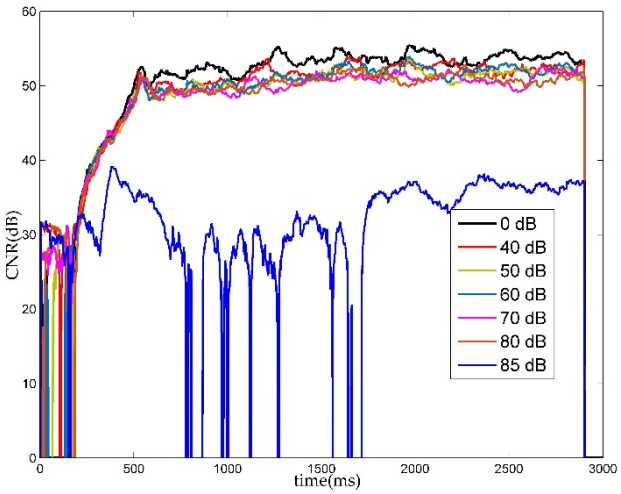

Fig. 7 The tracking CNRs after sweep interference suppression

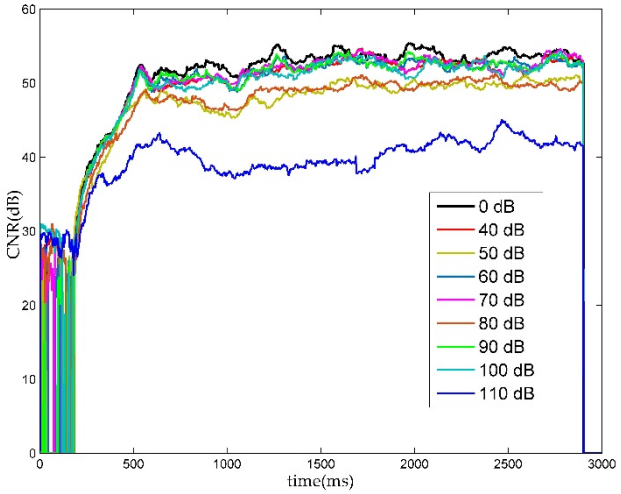

Fig. 8 The tracking CNRs after pulse interference suppression

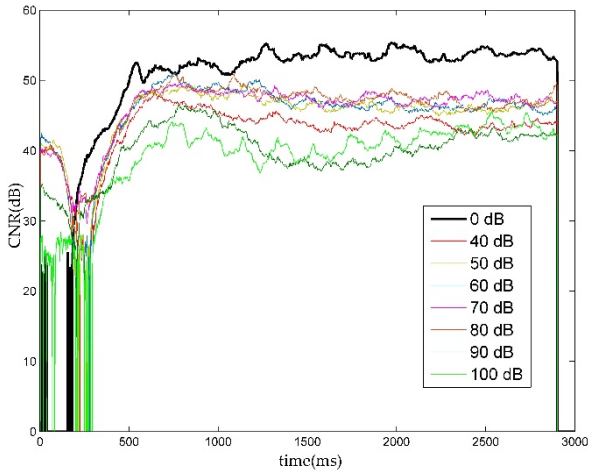

Fig. 9 The tracking CNRs after single-tone interference suppression

As shown in Fig. 7, we can conclude that the attenuation of CNR at the receiver end is less than 3 dB for sweep interference whose ISR is no more than 80 dB. For pulse interference whose ISR is under 100 dB, the attenuation of CNR is less than 6 dB, as shown in Fig. 8. As shown in Fig. 9, the attenuation of CNR is less than 8 dB for single-tone interference whose ISR is no more than 70 dB. The proposed method has good suppression performance for single-tone interference and excellent performance for sweep interference and pulse interference.

3.3 Comparison with Other Methods

In this subsection, we compare the anti-jamming performance of the proposed scheme with that of frequency domain adaptive filtering, adaptive FIR filtering and a code-aided technique. The main comparison indicator is the tracking CNR of the receiver after anti-jamming. We compare the corresponding CNR results obtained by the receiver after each method suppresses interference. The interference is single-tone interference with an ISR of 70 dB, and the basic parameters and jamming parameters of the simulation are shown in Table 1 and Table 2, respectively.

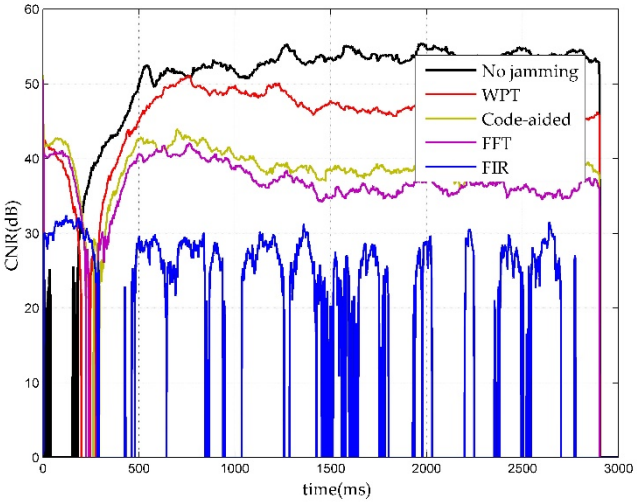

Fig. 10 Tracking CNRs for each method

We calculate the corresponding CNR of each method after suppressing interference. As shown in Fig. 10, the proposed method has a smaller attenuation of CNR of approximately 7dB. The frequency domain adaptive filtering and the code-aided technique have greater loss of tracking CNR after suppressing interference of 15 dB and 16 dB, respectively. The attenuation of CNR of the adaptive FIR filtering is the largest and is seriously deteriorated, indicating that this method cannot effectively filter out the interference.

4. Conclusion

In this paper, a GNSS interference suppression technology based on wavelet packet transform is proposed. First, the differences in different types of interference suppression performance are analyzed by simulation, and then the anti-jamming performance is comprehensively evaluated according to the acquisition results and the CNR of the receiver. Finally, we compare the scheme with some typical anti-interference methods. Comprehensive simulation results show that the proposed method can effectively suppress various types of interference, with strong adaptive ability and excellent performance.

References

[1] Kaplan, E.D., Hegarty, C.J. Understanding GPS: principles and applications Second Edition. In Artech House, 2006, p. 3-8.

[2] Borio, D., Camoriano, L., Savasta, S., Presti, L.L. Time-frequency excision for GNSS applications. IEEE Systems Journal. Vol. 2 (2008) No. 1, p. 27-37.

[3] Mosavi, M., Shafiee, F. Narrowband interference suppression for GPS navigation using neural networks. GPS solutions. Vol. 20 (2016) No. 3, p. 341-351.

[4] Poor, H.V. Active interference suppression in CDMA overlay systems. IEEE Journal on Selected Areas in Communications. Vol. 19 (2001) No. 1, p. 4-20.

[5] Mengüç, E.C., Acır, N. A generalized Lyapunov stability theory-based adaptive FIR filter algorithm with variable step sizes. Signal, Image and Video Processing. Vol. 11 (2017) No. 8, p. 1567-1575.

[6] Masry, E. Closed-form analytical results for the rejection of narrow-band interference in PN spread-spectrum systems-Part I: Linear prediction filters. IEEE Transactions on Communications. Vol. 32 (1984) No. 8, p. 888-896.

[7] Masry, E. Closed-form analytical results for the rejection of narrow-band interference in PN spread-spectrum systems-Part II: Linear interpolation filters. IEEE transactions on communications. Vol. 33 (1985) No. 1, p. 10-19.

[8] Wei, Y., Yan, Z. Variable tap-length LMS algorithm with variable tap-length adaptation step size. Chinese Control and Decision Conference (CCDC). Yinchuan, China, May 28, 2016, p. 3748-3751.

[9] Maraş, M., Ayvaz, E.N., Özen, A. A novel adaptive variable forgetting factor RLS algorithm. 26th Signal Processing and Communications Applications Conference (SIU). Cesme, Izmir, May 2-5, 2018, pp. 1-4.

[10] Chien, Y.-R., Huang, Y.-C., Yang, D.-N., Tsao, H.-W. A novel continuous wave interference detectable adaptive notch filter for GPS receivers. 2010 IEEE Global Telecommunications Conference GLOBECOM. Miami, FL, USA, pp. 1-6.

[11] Yin, F., Zhang, F. A Novel Blind Subspace Code-Aided Rejection of Narrowband Interference in CDMA Systems-Part I: Closed-Form Analytical Results. 7th International Conference on Wireless Communications, Networking and Mobile Computing. Wuhan, China, September 23-25 2011, p. 1-4.

[12] Yin, F., Zhang, F. A Novel Blind Subspace Code-Aided Rejection of Narrowband Interference in CDMA Systems-Part II: Adaptive Implementation. 7th International Conference on Wireless Communications, Networking and Mobile Computing. Wuhan, China, September 23-25 2011, pp. 1-4.

[13] Chen, X., Guo, W., Zheng, Y. Frequency domain interference suppression in a DSSS system. 2002 international conference on communications, circuits and systems and west sino expositions. Chengdu, China, 29 June-1 July 2002, p. 247-251.

[14] Capozza, P.T., Holland, B.J., Hopkinson, T.M., Landrau, R.L. A single-chip narrow-band frequency-domain excisor for a global positioning system (GPS) receiver. IEEE Journal of Solid-State Circuits. Vol. 35 (2000) No. 3, p. 401-411.

[15] Borio, D., Camoriano, L., Savasta, S., Presti, L.L. Time-frequency excision for GNSS applications. IEEE Systems Journal. Vol. 2 (2008) No. 1, p. 27-37.

[16] Oppenheim, A.V. Discrete-time signal processing. Pearson Education India. 1999, p. 436-451.

[17] Percival, D.B., Walden, A.T. Wavelet methods for time series analysis. Cambridge university press, 2006, p. 80-103.

[18] Wang, W., Guo, M., Chen, J.B. A New Narrowband Interference Mitigation Algorithm Based on Adaptive Wavelet Packet Decomposition. Fourth International Conference on Instrumentation and Measurement, Computer, Communication and Control. from September 18-20 2014, Harbin, China, pp. 6-11.

[19] Yang, W., Bi, G. Adaptive wavelet packet transform-based narrowband interference canceller in DSSS systems. Electronics Letters. Vol. 33 (1997) No. 14, p. 1189-1190.

[20] Pardo, E., Rodriguez-Hernandez, M.A., Pérez-Solano, J.J. Narrowband interference suppression using undecimated wavelet packets in direct-sequence spread-spectrum receivers. IEEE transactions on signal processing. Vol. 54 (2006) No. 9, p. 3648-3653.

[21] Wang, P., Wang, Y., Cetin, E., Dempster, A.G., Wu, S. GNSS Jamming Mitigation Using Adaptive-Partitioned Subspace Projection Technique. IEEE Transactions on Aerospace and Electronic Systems. Vol 55 (2018) No. 1, p. 343-355.